Journal of Applied Polymer Science

Modeling of the Degradation Kinetics of Biodegradable Scaffolds: The Effects of the Environmental Conditions

Marcin K. Heljak, Wojciech Swieszkowski, Krzysztof Jan Kurzydlowski
Faculty of Materials Science and Engineering, Warsaw University of Technology, Wołoska 141, Warsaw 02-507, Poland
Correspondence to: W. Swieszkowski (E-mail: wswieszk@inmat.pw.edu.pl)

ABSTRACT: The rate of hydrolytic degradation of tissue-engineered scaffolds made from bioresorbable polyesters is dependent on several factors. Some are related to the properties of the degrading polymeric material, but others are related to the geometry of the porous structure and the operating environment. It is well known that the rate of hydrolytic degradation of a given object, porous or nonporous, is lower when it is exposed to dynamic conditions, a flowing medium, than when it operates in static conditions. The most likely reason is the more efficient removal of the acidic degradation products from the vicinity of the polymeric material when it is operating in a flowing medium. In this article, we present a new phenomenological reaction–diffusion model of aliphatic polymer degradation. The model can be used to predict the significance of various factors in *in vitro* degradation tests, with particular reference to the flow of the degradation medium, and the frequency of medium replacement in the case of static conditions. The developed model was used to simulate the degradation of poly(DL-lactide-*co*-glycolide) scaffolds with different porosities subjected to static and dynamic testing conditions. The results confirm that the porosity of the scaffold had a significant influence on the degradation rate. It was shown that the combination of dynamic conditions and high porosity effectively reduced the mass loss and molecular weight loss of the degrading polymer. However, the effect of changes in the velocity of the flowing medium had a negligible effect on the rate of degradation. © 2014 Wiley Periodicals, Inc. J. Appl. Polym. Sci. **2014**, *131*, 40280.

KEYWORDS: biodegradable; biomedical applications; polyesters, theory, and modeling; porous materials

Received 15 July 2013; accepted 9 December 2013
DOI: 10.1002/app.40280

INTRODUCTION

The degradation of polymeric materials is a very important issue, not only from the point of view of polymer science, but it is crucial in the context of the majority of applications, especially in the biomedical field.[1,2] The majority of biodegradable polyesters used for orthopedic implants, including polylactide, polyglicolide, and their copolymers, suffer from *in situ* hydrolytic degradation in aquatic environments.[3,4] The resulting changes in the biophysical and biochemical properties of the polymers have a significant effect on the behavior of tissue-engineered components.

Hydrolysis is the dominant mechanism in the degradation of bioresorbable polyesters. Almost immediately after a polymer is placed into an aquatic environment, water molecules diffuse into the polymeric matrix. After some time, a large concentration of water molecules accumulates in the material. The water molecules reduce the strength of the chemical bonds of the polymeric chains. This causes them to divide into water-soluble shorter chains (oligomers and monomers) characterized by carboxylic ends, which are known to autocatalyze ester hydrolysis. These oligomers and monomers are able to diffuse inside the polymer matrix. The chain scissions inside the polymer matrix cause a reduction in the molecular weight of the polymer. The water-soluble monomers that are located near to the surface of the implant can leach out before total degradation occurs, whereas those that are located deep inside the polymer matrix remain entrapped and contribute to the autocatalytic effect.[5,6] This causes the degradation of large-size devices to proceed heterogeneously and to occur more rapidly internally than at the surface.

The degradation process of polyesters is influenced by a variety of specific physical factors, one of which is the degree of crystallization. The chain cleavage increases the mobility of the polymer chains, and this facilitates crystallization. The resulting crystalline phase, in turn, becomes more resistant for hydrolysis. The geometry of a degrading component affects monomer diffusion inside the polymer matrix and thereby influences the rate of degradation.[7] Other significant factors include the water content, the diffusion coefficients of polymer, the concentration of degradation products, and the chemical composition of the operating environment.[5,8]

There have been only a few reports that show how environmental conditions influence the degradation rate of aliphatic polymers.[9,10] Oh et al.[11] discussed the effect of the pH of the medium on the degradation behavior of tissue-engineered poly(DL-lactide-*co*-glycolide) (PLGA) scaffolds. The phosphate-buffered saline (PBS) solution used as the degradation medium was changed daily to maintain a near constant pH or less often to allow the formation of an acid caused by the degradation of PLGA and to lower the pH. The degradation of the scaffolds was quantified in terms of changes in the dimensions, molecular weight, mechanical properties, and scaffold morphology. The results reveal that the maintenance of the initial medium during the degradation test led to more rapid scaffold degradation than when the medium was replaced on a daily basis. It appeared that carboxylic acids released into the degradation medium acted as a catalyst and thus accelerated polymer degradation. The conclusion was drawn[11] that the environmental conditions, including acid accumulation in the medium, significantly affected the degradation behavior of the PLGA scaffolds.

Further evidence of the importance of the pH of the medium and the frequency of its replacement was reported by Bramfeldt et al.[12] They showed that an increase in the frequency of medium replacement resulted in a noticeable reduction in the rate of degradation.

In the work of Agrawal et al.,[13] the degradation under conditions of fluid flow was studied with special focus on the permeation through porous structures. The study suggested that tissue-engineered scaffolds subjected to flow conditions exhibited a slower rate of degradation and provided better mechanical support for a longer periods of time than those degraded under static conditions. This could be explained by the continuous removal of the degradation products from the material in a flowing medium. The progress in the experimental studies of the biodegradation of polymers has stimulated efforts to model this phenomenon. In the majority of the models of polymer degradation, the impact of the environment on the polymer degradation rate was assumed to be negligible. Consequently, the significance of the frequency of medium replacement and the influence of the medium flow was disregarded, despite the evidence of the experimental findings. Particularly noteworthy is the work by Mohammadi and Jabbari,[14] who developed the kinetic Monte-Carlo model for polymer scaffold degradation, which includes the effect of the scaffold porosity on the rate of degradation resulting from the acidity of the environment associated with the concentration of the oligomers. The authors reported that the higher the porosity of the scaffold was, the lower the rate of degradation, the loss of mass, and the concentration of oligomers in the scaffold pores were. However, the diffusion of the oligomers was not analyzed in this study. Models of polymer hydrolytic degradation are generally divided into two categories: phenomenological and mechanistic.[15] Phenomenological models,[16,17] are based on diffusion–reaction equations, where the reaction component accounts for the hydrolysis, and the diffusive part of the equation accounts for the diffusion of the degradation products. Typical examples of mechanistic modeling are the Monte-Carlo and cellular automata models.[18] Although the progress made with the development of existing models of polymer degradation are recognized, we considered that more factors could be taken into account to model the degradation of polymeric scaffolds for tissue engineering.

In this article, we report on efforts to develop a new phenomenological reaction–diffusion numerical model of aliphatic polymer degradation. Our goal was to produce a model that could predict the process of scaffold degradation and take into account the effect of the environmental conditions, particularly dynamic or static degradation, the frequency of medium replacement, and the geometry of the components.

EXPERIMENTAL

Model Formulation

The developed model of the degradation of aliphatic polymers is based on the concept presented by Wang et al.[16] with major simplifications proposed in this article. In particular, the water diffusion is not considered in the model; we assumed that the polymer bulk was instantly saturated by water. The autocatalytic degradation process was modeled with the following system of reaction–diffusion equations:

$$\frac{\partial C_e}{\partial t} = -\left(k_1 C_e + k_2 C_e C_m^n\right) \tag{1}$$

$$\frac{\partial C_m}{\partial t} = k_1 C_e + k_2 C_e C_m^n + \underset{x_i}{\text{div}} \left\{ D \underset{x_i}{\text{grad}} \left(C_m\right) \right\} \tag{2}$$

$$D = D_0 \left[1 + \alpha\left(1 - \frac{C_m + C_e}{C_{e0}}\right)\right] \tag{3}$$

where C_e is the ester bond concentration; C_{e0} is the initial ester bond concentration, which is related to the molecular weight; D is the diffusion coefficient of the monomers in the polymer matrix; D_0 is the initial diffusion coefficient for monomers in the nondegraded polymer matrix; t is the time of degradation; div and grad are divergence and gradient, respectively, of the monomer concentration at a given location $(x_1, x_2, \ldots, x_n)$; and C_m is the monomer concentration, which could also be treated as the concentration of the degradation products. At the initial state of the degradation, C_m is assumed to be equal to zero; k_1 and k_2 are the phenomenological reaction rate constants. The power n accounts for the dissociation of the acidic end groups. A special parameter (α) was used to compute the effective diffusivity of the monomers. The first term in eq. (1) is related to the nonautocatalytic reaction of hydrolysis, whereas the second term includes the acidic-catalyzed hydrolysis, which is caused by presence of the monomers and the other polymer degradation products. Equation (2) is the reaction–diffusion equation and is composed of the source term responsible for the monomer formation and the diffusion term related to monomer transport inside the polymer bulk.

In numerical analyses, it is convenient to use a nondimensional form of the previous equations, which provides results that are not specific to the dimensions and material properties. If the reaction rate of the catalyzed hydrolysis (k_2) is used as the reference, the nondimensional variables are as follows:

$$\overline{C}_e=\frac{C_e}{C_{e0}},\ \overline{C}_m=\frac{C_m}{C_{e0}},\ \overline{x}_i=\frac{x_i}{l},\ \overline{t}=\left(k_2 C_{e0}^n\right)t,\ \overline{k}_1=\frac{k_1}{k_2 C_{e0}^n},\quad \overline{D}=\frac{D_0}{C_{e0}^n k_2 l^2}\left[1+\alpha\left(1-\frac{C_m+C_e}{C_{e0}}\right)\right] \tag{4}$$

where l is the characteristic length of the object subjected to degradation and t is the time of degradation.

Equations (1) and (2) can then be rewritten as follows:

$$\frac{\partial \overline{C}_e}{\partial \overline{t}}=-\left(\overline{k}_1\overline{C}^{1}{}_e+\overline{C}_e\overline{C}_m^n\right) \tag{5}$$

$$\frac{\partial \overline{C}_m}{\partial \overline{t}}=\overline{k}_1\overline{C}_e+\overline{C}_e\overline{C}_m^n+\underset{\overline{x}_i}{\mathrm{div}}\left\{\overline{D}\ \underset{\overline{x}_i}{\mathrm{grad}}\left(\overline{C}_m\right)\right\} \tag{6}$$

The ester bond concentration is related to the molecular mass of the polymer matrix and is subjected to hydrolytic degradation in the following manner:[19,20]

$$\overline{M}=\overline{C}_e \tag{7}$$

where $\overline{M}$ is the normalized molecular weight. Normalization was made with respect to the initial values of the molecular weight and the concentration of ester bonds. Equations (5) and (6) should be supplemented with terms to account for the diffusion of monomers in the degradation medium, which is characterized by the different coefficient (D_{medium}). The nondimensional form of D_{medium} is given in eq. (8). Wang's model was modified to consider the influence of the environment on the rate of degradation. Equation (6) was rewritten to a form valid model for the degradation medium domain [eq. (9)]:

$$\overline{D}_{\mathrm{medium}}=\frac{D_{\mathrm{medium}}}{C_{e0}^n k_2 l^2} \tag{8}$$

$$\begin{cases}\dfrac{\partial \overline{C}_m}{\partial \overline{t}}=\overline{k}_1\overline{C}_e+\overline{C}_e\overline{C}_m^n+\underset{\overline{x}_i}{\mathrm{div}}\left\{\overline{D}\ \underset{\overline{x}_i}{\mathrm{grad}}\left(\overline{C}_m\right)\right\} & \text{for } \overline{x}_i\in\Omega_{\mathrm{polymer}}\\ \dfrac{\partial \overline{C}_m}{\partial \overline{t}}=\underset{\overline{x}_i}{\mathrm{div}}\left\{\overline{D}_{\mathrm{medium}}\ \underset{\overline{x}_i}{\mathrm{grad}}\left(\overline{C}_m\right)\right\} & \text{for } \overline{x}_i\in\Omega_{\mathrm{medium}}\end{cases} \tag{9}$$

where $\Omega_{\mathrm{polymer}}$ is the degraded polymer domain.

The degradation process occurs because the monomers diffuse from the bulk polymer into the surrounding medium. In the majority of degradation experiments, the degradation medium (PBS, simulated body fluid (SBF), or Dulbecco's modified Eagle's medium (DMEM)) is replaced at predetermined intervals, so he released monomers are dissolved and then distributed homogeneously in the pores of the scaffold. The presented model enables the degradation process under conditions of periodic replacement of the degradation medium (static degradation) or with a flowing medium (dynamic degradation) to be simulated. In the case of dynamic degradation, the medium flow elutes the degradation products at a specific rate, so the monomer concentration in the degradation medium domain (Ω_{medium}) was assumed to be permanently equal to zero [eq. (10)]. In the case of static degradation, the monomer concentration in the medium domain is set to zero only at the predetermined time points $\{t_{1\_\mathrm{rep}}, t_{2\_\mathrm{rep}}, \ldots, t_{n\_\mathrm{rep}}\}$, which correspond to the times of medium replacement. Except for the listed time points eq. (9) is valid for the degradation medium domain:

$$x\in\Omega_{\mathrm{medium}}:\begin{cases}\text{Dynamic}: C_m(x,t)=0 \text{ for } t\in[0,t_{\mathrm{finish}}]\\ \text{Static}: \begin{cases}t=\left\{t_{1_{\mathrm{rep}}},t_{2_{\mathrm{rep}}},\ldots,t_{n_{\mathrm{rep}}}\right\}: C_m(x,t)=0\\ t\neq\left\{t_{1_{\mathrm{rep}}},t_{2_{\mathrm{rep}}},\ldots,t_{n_{\mathrm{rep}}}\right\}: \dfrac{\partial C_m}{\partial t}=\underset{x_i}{\mathrm{div}}\left\{D_{\mathrm{medium}}\ \underset{x_i}{\mathrm{grad}}\left(C_m\right)\right\}\end{cases}\end{cases} \tag{10}$$

where t_{finish} is time at the end of degradation.

Polymer Mass Loss

It is generally accepted that the polymer's loss of mass is caused by the loss of degradation products, oligomers, and monomers into the degradation medium. The final stage of the degradation process occurs when the mass loss is the consequence of the physical disintegration of the polymer. It was assumed that the mass loss is a function of the monomer concentration inside the polymer matrix. Until the monomer concentration reaches its maximum level, the mass loss is assumed to be zero:

$$\frac{\partial \overline{m}(\overline{t},\overline{x})}{\partial \overline{t}}=\begin{cases}0, & \overline{t}\le\overline{t}_{\max}\\ -\overline{k}_m\left(\overline{C}_m^{\max}\right)^2 if & \overline{t}\ge\overline{t}_{\max}\end{cases} \tag{11}$$

where m is the polymer mass, $t_{\max}$ is the normalized time at which the monomer concentration reaches its maximal value, k_m is the normalized coefficient of mass loss, and $\overline{C}_m{}^{\max}$ is the normalized maximal value of the monomer concentration. As soon as the maximum level is achieved, the rate of mass loss is directly proportional to the maximum value of the monomer concentration. This is justified by the fact that the accumulation of the degradation products inside the polymer matrix progresses to a point where the number of polymer chains reaches a peak value. From this point, the chains dissolve into oligomers and monomers and diffuse out of the polymer matrix. This activity corresponds to the inflexion in the mass loss curve.[5,21] Equation (11) is integrated during the postprocessing stage of the simulation, by which time the maximal monomer concentrations should be known.

Because bulk degradation is considered in the model, the changes in the geometry of object subjected to degradation are disregarded.

Reanalysis of the Data Obtained by Agrawal et al.[13]

Agrawal et al.[13] carried out degradation experiments on PLGA copolymer (with an inherent viscosity of 0.69 dL/g) using three groups of scaffolds with various degrees of porosity (high porosity = 92%, medium porosity = 87%, and low

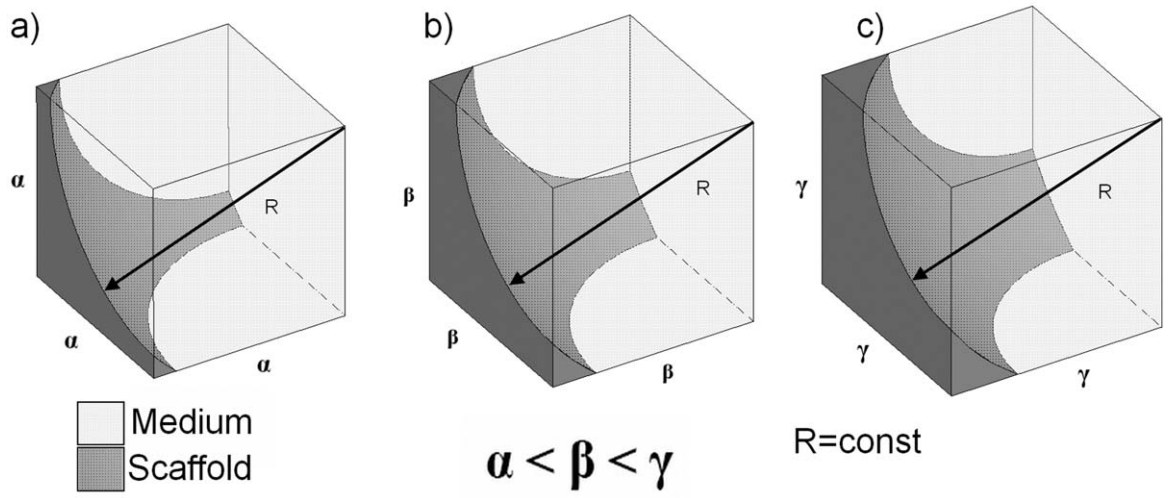

Figure 1. Representative scaffold cell geometries for (a) 92, (b) 87, and (c) 80% porosity. α, β, and γ represent the sizes of the representative scaffold cells, and R is the pore radius for all of the scaffolds (180 μm).

porosity = 80%). Each type of scaffold was analyzed in flowing and static media. A constant flow of PBS at pH 7.4 and 37°C was assumed with a flow rate of 250 μL/min. In the case of both static and dynamic degradation, the PBS was replaced every 3.5 days to prevent significant changes in the acidity. The scaffolds were fabricated with a vibrating particle technique; this means that their degree of porosity depended mainly on the polymer/salt ratio. Salt particles with diameters in the range 250–500 μm were used as the porogen. This led us to conclude that the pore size was the same for each case of scaffold porosity. Here, we use our model to reanalyze their experimental data for scaffold degradation.

RESULTS AND DISCUSSION

Geometrical Model of Polymeric Scaffolds

The geometry of the representative scaffold cells is shown in Figure 1. The variation of porosity was achieved by variation of the wall thickness; this ensured that the pore diameter remained constant.

Numerical Procedure

The system of differential equations [eq. (9)] was solved with a standard Euler scheme, whereby the diffusion–reaction equation was integrated with a finite element method at each time step of the Euler scheme. The model was implemented with ANSYS Parametric Design Language (ANSYS version 11). The finite element method (FEM) model of the representative cell was generated with ANSYS Mechanical APDL version 11 code. The cell geometry was meshed with a 4200 four-node tetrahedral finite element (SOLID70 used in thermal analysis; Figure 2).

On the representative cell walls, the periodic boundary conditions were imposed in such a way that the monomer concentration gradient was assumed to be zero. The simulation results were obtained with the following nondimensional model parameters and initial conditions: $\overline{C}_{e0} = 1$, $\overline{C}_{m0} = 0$, $\overline{t} = 6$, $\overline{k}_1 = 8 \times 10^{-4}$, $\overline{D}_0 = 0.1$, $\overline{D}_{\text{medium}} = 10 \times 10^4$, $\overline{r} = 2$, $\overline{k}_m = 11$, and $n = 0.2$, where $\overline{r}$ is the normalized radius of the pore sphere. The parameters $\overline{k}_1$, $\overline{D}_0$, $\overline{D}_{\text{medium}}$, and n were taken arbitrarily to provide initial agreement with the experimental results.

Simulation Results

The simulation results are shown in Figure 3 in such a way that enables comparison with the experimental data obtained by Agrawal et al.[13]

The results indicate a strong autocatalytic effect during degradation. Scaffolds with a lower porosity (thicker pore walls) degraded more rapidly. This was the result of the shortened polymeric chains with acid end groups, which are known to autocatalyze ester hydrolysis. As these could not diffuse out sufficiently and rapidly, they accumulated within the polymer matrix (Figure 3).[6] The influence of the acidity of the surrounding medium on the degradation rate was clearly confirmed. The group of scaffolds operating in the dynamic medium degraded

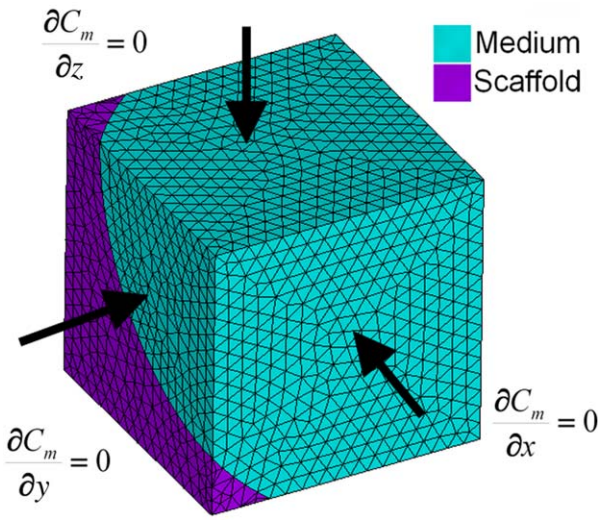

Figure 2. Finite element method model of a representative cell. [Color figure can be viewed in the online issue, which is available at wileyonlinelibrary.com.]

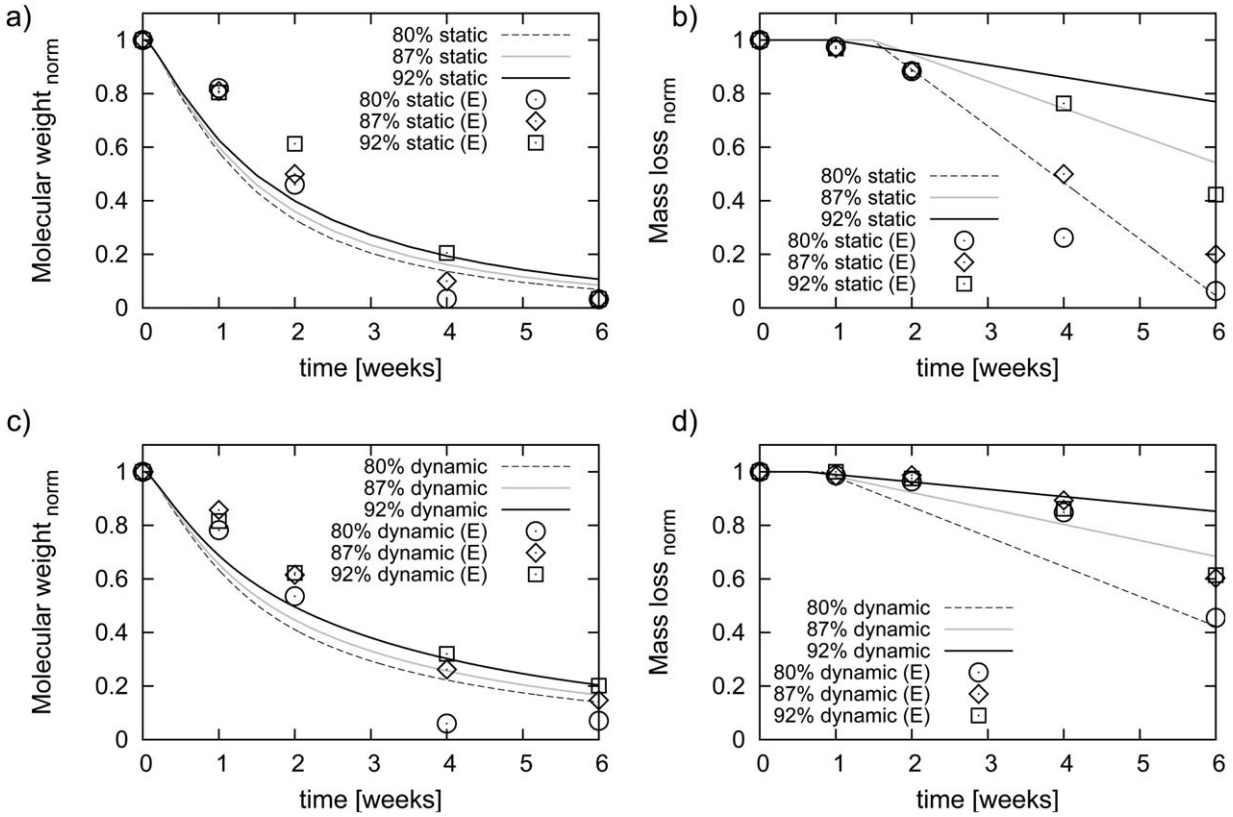

Figure 3. Comparison of the simulation results and the experimental data from Agrawal et al.[13] for the average molecular weight under (a) static and (c) dynamic conditions and for the polymer mass loss under (b) static and (d) dynamic conditions as functions of the degradation time. *E* represents the values measured in the experiments. "norm" means the normalized values which they are distinguished by overbars in text.

significantly more slowly than those exposed to the static medium (Figure 4). This could be explained by the efficient removal of the acidic degradation products from the vicinity of the polymer matrix. This significantly improved monomer release into the medium and, at the same time, reduced the monomer accumulation inside the scaffold (Figure 3). In the case of the dynamic mode of degradation, the degradation products were advected because of the specific rate of the medium's motion, so an extra term may be added to the right hand side (RHS) of eq. (9). However, the assumption was made that the effect of differences in the advection velocities (resulting from different scaffold porosities) on the rate of degradation was negligible. The rate of monomer advection was many times higher than the rate of monomer diffusion. It follows that significantly different advection velocities should yield similar effects. The validity of this assumption was confirmed by the results of the simulation. The fit of the modeled predictions to the experimental results obtained by Agrawal et al.[13] was very

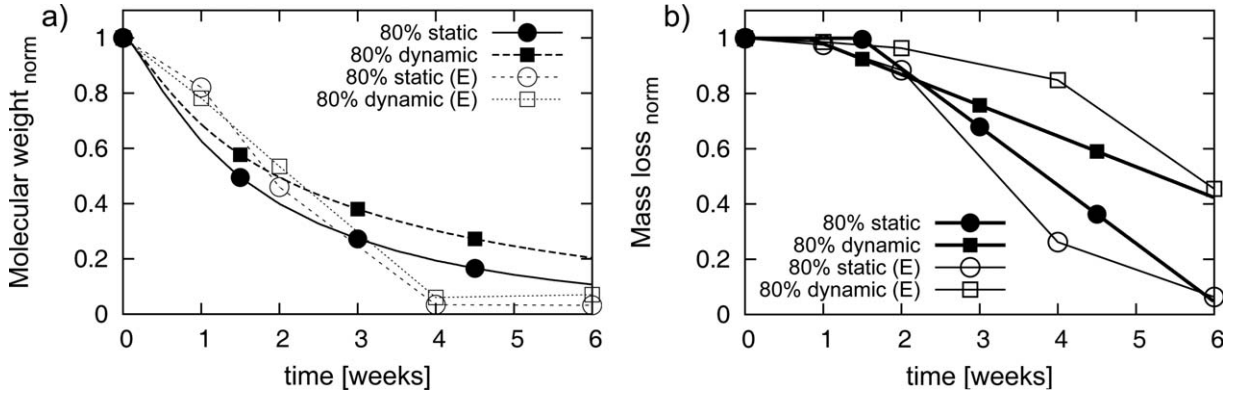

Figure 4. Demonstration of the effects of the environmental conditions on the degradation rate. The model prediction and experimental data from Agrawal et al.[13] for the 80% scaffold porosity case were compared: (a) the average molecular weight under static and dynamic conditions and (b) the polymer mass loss under static and dynamic conditions. *E* represents the values measured in the experiments. "norm" means the normalized values which they are distinguished by overbars in text.

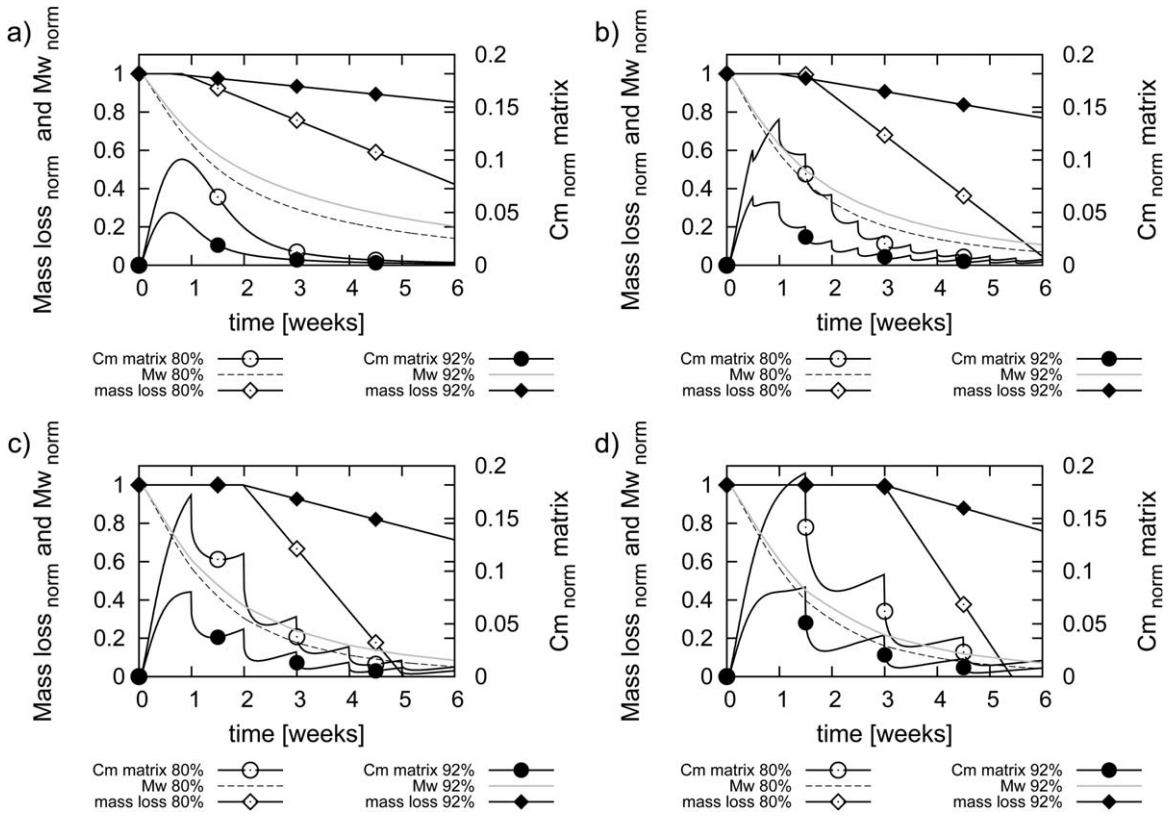

Figure 5. Monomer concentration inside the polymer matrix, average molecular weight (M_w), and mass loss as functions of the degradation time calculated for (a) dynamic degradation conditions, (b) static degradation conditions (with the medium replaced every 3.5 days), (c) static degradation conditions (with the medium replaced every 7 days), and (d) static degradation conditions (with the medium replaced every 10.5 days). "norm" means the normalized values which they are distinguished by overbars in text.

satisfactory. The agreement achieved between the experimental and simulation results for the mass loss proved the validity of eq. (11) used for the computation of the mass loss of the polymer.

The plot in Figure 5 highlights the interdependency between the mass loss, reduction in molecular weight, and concentration of degradation products inside the polymer matrix. The sawtooth-like shape of the curves of the monomer concentration in Figure 5 showed the effect of medium replacement at predetermined intervals. After the replacement, the gradient of monomer concentration at the polymer–medium interface increased significantly, and consequently, the monomer diffusion process was much more efficient. It was also evident that during dynamic degradation, the maximal monomer concentration in the medium was much lower than in the case of static degradation. Consequently, the less frequent renewal of the medium was, the more rapid the loss of molecular weight was.

Model Limitations

The porosity of the degraded scaffolds measured by Agrawal et al.[13] changed throughout the degradation process; however, the relationship between the degradation conditions and the scaffold porosity was not very evident. For this reason, the scaffold porosities were assumed to be constant in the reported work.

The molecular weight loss profile of the scaffolds with 80% porosity in both the dynamic and static situations varied somewhat from the experimental results The reason may have been that the geometry of the least porous scaffolds were changed in a significant manner.[13] The proposed model does not take into account any changes in the scaffold geometry during the period of degradation, and therefore, effects related to these changes have not been included.

Another limitation of the model is the inability to accurately calculate the molecular weight distribution at successive stages of the polymer degradation process, whereas the calculated average molecular weight is unable to distinguish between the number-average molecular weight and the weight-average molecular weight.

CONCLUSIONS

A mathematical model to simulate the degradation of biodegradable bulk-erosive porous devices has been proposed. The model takes into account the effects of the periodic replacement of the surrounding medium in the case of static degradation and the flow of the medium through the scaffold pores in the case of dynamic degradation.

The goal of the reported study was to highlight the significance of the environment in which a given device is subjected to degradation. The results of the simulations indicate that the rate of degradation was reduced when a scaffold was subjected to degradation in a dynamic medium. The presented results prove

that the rate of degradation was affected by the scaffold porosity, as it has been established that thicker pore walls induce stronger autocatalysis and, consequently, a higher rate of degradation.

The developed model of polymer degradation could be especially useful in predicting the biodegradation profiles of tissue-engineered scaffolds during *in vitro* cell culturing in bioreactors. The physiological environment that prevails inside a bioreactor can be characterized by different factors, including the temperature, the concentration of oxygen and carbon dioxide, and the mechanical stimuli that come from the environment. All of these factors potentially affect the rate of scaffold degradation. Although the mechanical properties of a bioresorbable scaffold are strongly dependent on the extent of scaffold degradation, the properties when it is implanted should match those of the host tissue as closely as possible.[22,23] The model of polymeric scaffold degradation presented in this article could effectively reduce the time needed for the selection of appropriate scaffold material and the appropriate conditions for tissue culturing.

ACKNOWLEDGMENTS

This work was supported by the Polish National Science Center through contract grant number 2011/01/B/ST8/07437.

REFERENCES

1. Swieszkowski, W.; Tuan, B. H. S.; Kurzydlowski, K. J.; Hutmacher, D. W. *Biomol. Eng.* **2007**, *24*, 489.
2. Moczulska, M.; Bitar, M.; Święszkowski, W.; Bruinink, A. *J. Biomed. Mater. Res. A* **2012**, *100*, 882.
3. Nair, L. S.; Laurencin, C. T. *Prog. Polym. Sci.* **2007**, *32*, 762.
4. von Burkersroda, F.; Schedl, L.; Göpferich, A. *Biomaterials* **2002**, *23*, 4221.
5. Grizzi, I.; Garreau, H.; Li, S.; Vert, M. *Biomaterials* **1995**, *16*, 305.
6. Wu, L.; Ding, J. *J. Biomed. Mater. Res. A* **2005**, *75*, 767.
7. Saito, E.; Liu, Y.; Migneco, F.; Hollister, S. J. *J. Acta Biomater.* **2012**, *8*, 2568.
8. Schliecker, G.; Schmidt, C.; Fuchs, S.; Wombacher, R.; Kissel, T. *Int. J. Pharm.* **2003**, *266*, 39.
9. Huang, Y.; Qi, M.; Zhang, M.; Liu, H.; Yang, D. T. *Nonferrous Metal. Soc.* **2006**, *16*, 293.
10. Kang, Y.; Xu, X.; Yin, G.; Chen, A.; Liao, L.; Yao, Y.; Huang, Z.; Liao, X. *Eur. Polym. J.* **2007**, *43*, 1768.
11. Oh, S.; Kang, S.; Lee, J. *J. Mater. Sci.: Mater. Med.* **2006**, *17*, 131.
12. Bramfeldt, H.; Sarazin, P.; Vermette, P. *J. Polym. Degrad. Stab.* **2008**, *93*, 877.
13. Agrawal, C.; McKinney, J.; Lanctot, D.; Athanasiou, K. *Biomaterials* **2000**, *21*, 2443.
14. Mohammadi, Y.; Jabbari, E. *Macromol. Theory Simul.* **2006**, *15*, 643.
15. Sackett, C. K.; Narasimhan, B. *Int. J. Pharm.* **2011**, *418*, 104.
16. Wang, Y.; Pan, J.; Han, X.; Sinka, C.; Ding, L. *Biomaterials* **2008**, *29*, 3393.
17. Chen, Y.; Zhou, S.; Li, Q. *J. Acta Biomater.* **2011**, *7*, 1140.
18. Chao, G.; Xiaobo, S.; Chenglin, C.; Yinsheng, D.; Yuepu, P.; Pinghua, L. *Mater. Sci. Eng. C* **2009**, *29*, 1950.
19. Han, X.; Pan, J. *Biomaterials* **2009**, *30*, 423.
20. Han, X.; Pan, J.; Buchanan, F.; Weir, N.; Farrar, D. *J. Acta Biomater.* **2010**, *6*, 3882.
21. Göpferich, A. *Biomaterials* **1996**, *17*, 103.
22. Hutmacher, D. W. *Biomaterials* **2000**, *21*, 2529.
23. Heljak, M. K.; Święszkowski, W.; Lam, C. X. F.; Hutmacher, D. W.; Kurzydłowski, K. J. *Int. J. Numer. Methods Biomed. Eng.* **2012**, *28*, 789.